LETTERS

Self-Assembling of Monolayer-Protected Gold Nanoparticles

Shaowei Chen[†]

Department of Chemistry and Biochemistry, Southern Illinois University, Carbondale, Illinois 62901-4409

Received: October 1, 1999; In Final Form: December 2, 1999

Self-assembling of monolayer-protected gold nanoclusters onto a gold electrode surface was reported. The particles were surface-active with multiple copies of peripheral thiol groups that resulted from an exchange reaction with alkanedithiols. Excessive dithiol and displaced thiol ligands were removed from the cluster exchange solution via liquid extraction using a hexane−methanol system. The self-assembling process appeared to be rather fast, similar to that for simple alkanethiols. The resulting particle adlayers exhibited discrete electron-transfer features that were ascribed to the quantized capacitance charging to the particle double layers. The electrode double-layer capacitance, evaluated from impedance measurements, also showed a modulation with electrode potentials. Consistent electron-transfer rate constants were obtained from the Laviron evaluation as well as from the impedance measurements. The electron-charging behaviors were also quite visible in aqueous media when the interparticle "void" space was filled up with low-dielectric organic adlayers. Technical implications of these particle assemblies were also discussed.

Organized architectures of nanometer-sized particles are attracting extensive attention in diverse fields, in part, because of the fundamental importance and technological implications involved in these ordered arrays of quantum dots.[1−10] The great application potentialities of metal nanoparticles as the building blocks for the construction of electronic nanodevices/nanocircuits have been partly motivated by the unique electronic/electrical properties associated with these artificial molecular entities. In particular, for metal nanoparticles that are passivated by a dielectric organic layer (or, *monolayer-protected clusters*, MPCs), the particles exhibit a (sub)attofarad molecular capacitance, which, upon the charging of a single electron, experience a rather substantial potential change (and vice versa), the so-called Coulomb staircase charging.[4,11−13] These discrete electron-charging behaviors have been observed at ambient conditions both in solutions of MPCs of relatively monodisperse cores[11,13] and with surface-immobilized MPCs.[12] The electrochemical

responses were found to be dependent upon a variety of factors, including the particle core size, monolayer thickness, and dielectric, as well as solvent properties.[11,13]

Understandably, the main technological challenge in the exploration of MPC potential applications as single-electron transistors[10] lies in the lack of efficient methods to assemble the particles into macroscopic well-ordered structures. There has been a great deal of research effort devoted to the development of new methodologies for the construction of particle-ordered assemblies.[1−7] Among them, a general strategy is to utilize (rigid) bifunctional ligands,[2−5] where a self-assembled monolayer is preformed with one end adsorbed onto a substrate surface and the other end used to anchor the particles.

For "naked" colloidal particles, the above sequential anchoring mechanism was rather efficient, for instance, by electrostatic interactions, covalent linkage, or sorptive interactions.[2−10] Typically, within hours the surface assemblies reached an equilibrium. However, for monolayer-protected particles (MPCs), there has been very limited success so far, probably due to the steric hindrance that rendered the process very tedious and

† Telephone: (618) 453-2895. Fax: (618) 453-6408. E-mail: schen@chem.siu.edu.

SCHEME 1: (A) Schematic of Self-Assembling of Surface-Active MPCs; (B) Hypothetical Surface Structures of the Adsorbed Particles; and (C) Equivalent Circuit (Randles circuit) for the Particle Surface Assemblies[a]
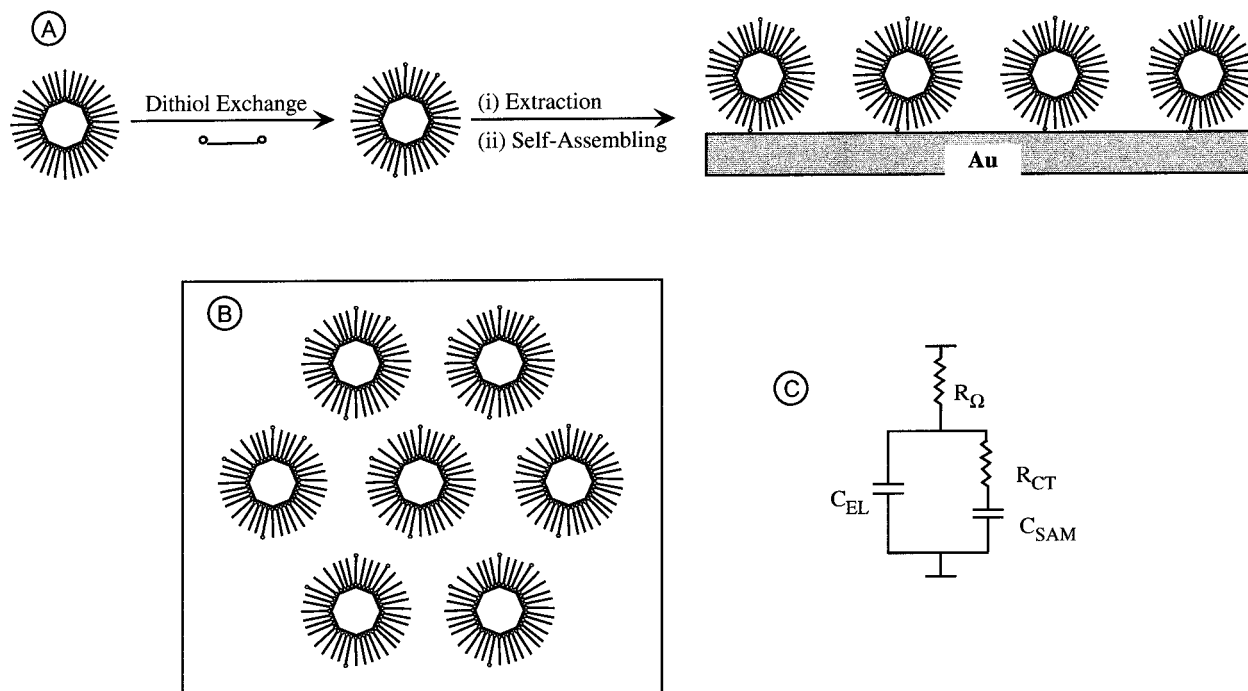
[a] R_Ω denotes the (uncompensated) solution resistance, R_{CT} is the charge-transfer resistance, and C_{SAM} and C_{EL} reflect the components of electrode double-layer capacitance from the electrode surface with and without adsorbed MPC molecules, respectively.

technically challenging. For instance, recently we described two routes to construct surface-ordered arrays of alkanethiolate-protected gold nanoparticles,[12] by using 4,4′-thiobisbenzenethiol (TBBT, $HS-C_6H_4-S-C_6H_4-SH$) as the linking ligands. The first approach entailed the anchoring of alkanethiolate-protected gold clusters onto a preformed TBBT monolayer on a gold electrode surface by ligand place-exchange; whereas in the second approach, a few copies of TBBT were initially incorporated into the Au cluster protecting monolayers in the de novo synthesis, rendering the particles surface-active (with free thiols), which were then self-assembled onto gold electrodes surfaces. Both approaches resulted in modest surface-coverage of nanoparticle assemblies, as characterized electrochemically; however, the process was rather time-consuming (about 1 week). In particular, the second approach was complicated by the effect of monolayer mixture on particle size and size dispersity.[12,13]

In this letter, we describe a much-improved method to achieve efficient self-assembling of nanoparticles and the results of electrochemical studies. Here, we utilize alkanedithiols as the bifuncional linkers by taking advantage of the recent progress in the study of ligand place-exchange reactions on MPCs.[14] Specifically, multiple copies of dithiols were exchanged into the protecting monolayers of alkanethiolate MPCs,[14] rendering the resulting particles surface-active with free thiols on the outer peripheral surface. Excessive dithiols and displaced thiols were then removed by liquid extraction from the exchange solution, and self-assembled monolayers of MPCs could then be constructed by immersing a cleaned (gold) electrode into the resulting solution of surface-active particles (outlined in Scheme 1). One of the apparent advantages of the current approach was to keep the thiol-terminated MPCs in solution so as to prevent undesired particle cross-linking that had been observed previously with dithiol-functionalized particles.[16]

We took 1-hexanethiolate-protected gold (C6Au) clusters and 1,6-hexanedithiol (HSC6SH) as the illustrating example. Here the C6Au particles were synthesized by the Schiffrin reaction[17]

and partially fractionated by a mixture of toluene and ethanol (1:2 v:v).[18] Then varied copies of dithiol ligands were exchanged into the particle-protecting monolayers.[14] In a typical reaction, 25 mg of C6Au clusters and 3 μL HSC6SH were co-dissolved in 10 mL of hexane (the initial ratio of HSC6SH:C6S ≈ 1:2, and cluster concentration approximately 50 μM), and the solution was under constant stirring for about 24 h. To remove excessive and displaced thiol ligands, instead of drying the samples (a procedure that typically resulted in aggregation of particles due to the intercalation and cross-linking by the dithiols[16]), we employed liquid extraction. Since alkanethiolate-protected gold particles are soluble only in apolar solvents such as hexane but not in polar media (e.g., alcohols), we chose methanol for the extraction, also because methanol and hexane are only slightly miscible. Complete removal of free thiol ligands was effected by repeated extractions. This was characterized by proton NMR spectroscopy, where an aliquot of solution was dried and the sample was then rinsed with deuterized solvents (e.g., C_6D_6). Since the particle aggregates were not soluble, any free ligands would be easily detected by NMR measurements (according to the previous study of MPC ligand place-exchange reaction,[14] the final monolayer composition corresponded to roughly 20% exchange, i.e., approximately 10 free thiols per MPC). The resulting solution was then diluted/concentrated to a desired concentration for monolayer fabrication.

The construction of self-assembled monolayers of nanoparticles was relatively straightforward, where a cleaned (polycrystalline) gold disk electrode sealed in glass tubing was immersed into the above-obtained solution (~50 μM) of surface-active particles for, typically, 18 h, just like simple alkanethiols.[15] The electrode was then rinsed with copious hexane to remove loosely bound particles, dried in a N_2 stream, and transferred to an electrolyte solution for electrochemical measurements.

Figure 1 shows the cyclic (A, CV) and differential pulse (B, DPV) voltammograms (BAS 100B/W Electrochemical Ana-
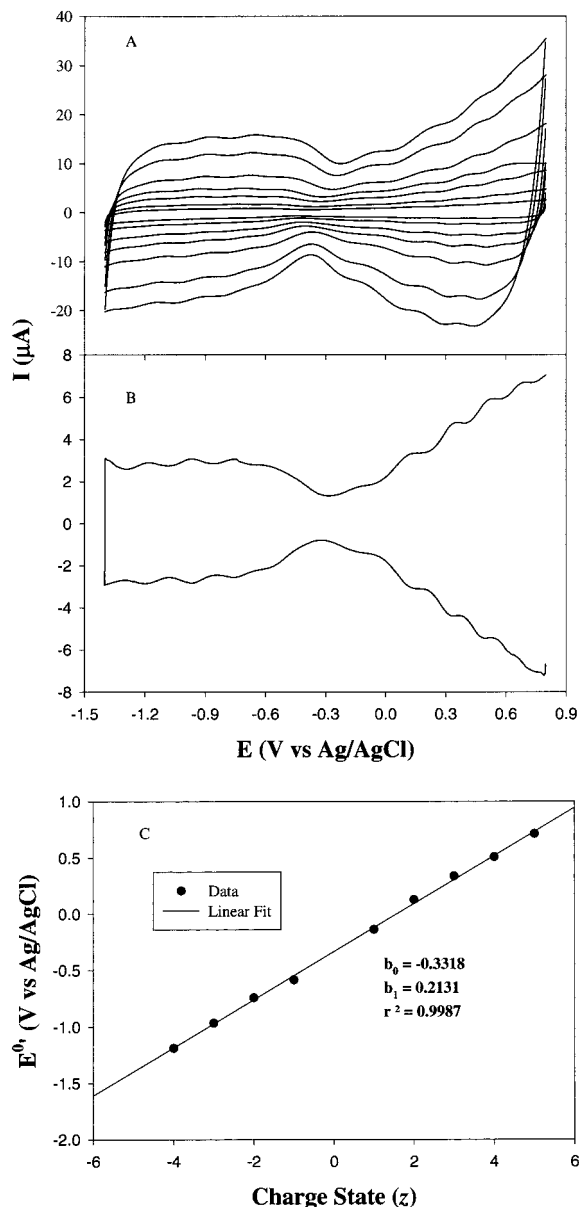
Letters

J. Phys. Chem. B, Vol. 104, No. 4, 2000 **665**

Figure 1. Cyclic (A, CV) and differential pulse (B, DPV) voltammograms of a self-assembled monolayer of C6Au particles onto a gold electrode surface in CH$_2$Cl$_2$ containing 0.1 M TBAP. CV sweep rates increase from 100 to 200, 400, 600, 902, 1505, and 2000 mV/s; and in DPV, the DC potential sweep rate 10 mV/s, pulse amplitude 50 mV. Electrode area 0.116 cm^2. (C) Plot of variation of charging formal potentials with MPC charge state (z-plot). Data obtained from DPV measurements.

lyzer) of a C6Au MPC monolayer on a gold electrode surface (linked by 1,6-hexanedithiols) in a CH$_2$Cl$_2$ solution containing 0.1 M tetra-*n*-butylammonium perchlorate (TBAP). One can see that there are multiple well-defined voltammetric waves within the potential range of −1.4 to +0.8 V. These were ascribed to the discrete charging of the adsorbed particle double layers, namely, the electrochemical Coulomb staircase charging.[11−13] The peak positions were also very consistent with those observed with the C6Au MPCs in solutions, indicating that the quantized charging behaviors were similar between solution-phase and surface-confined MPCs.[11−13] The appearance of discrete charging waves also suggests that the lateral interparticle resistance must be much greater than the charge-transfer resistance, R$_{CT}$ (Scheme 1C), consistent with our previous studies.[12] It has been shown[11c] that the formal potential of a quantized capacitance charging peak in which the charge state changes from z to z −

1 is

$$E^{\circ}_{z,z-1} = E_{PZC} + \frac{(z - 1/2)e}{C_{MPC}} \quad (1)$$

where E_{PZC} is the potential of zero charge, C_{MPC} is the MPC capacitance, and e is the electronic charge. Equation 1 dictates a linear relationship between the formal potentials and the charge states of the MPCs if C_{MPC} is independent of electrode potential, and from the slope and intercept one can evaluate C_{MPC} and E_{PZC}, respectively. Figure 1C shows the variation of formal potentials with charge states which exhibits good linearity, as evidenced by linear regression analysis. From the slope one can estimate that C_{MPC} = 0.75 aF, corresponding to an *effective* core radius of approximately 0.99 nm (assuming a dielectric constant of 3 for the C6 protecting monolayer and the fully extended chainlength of C6, 0.67 nm),[11c] and from the intercept, E_{PZC} = −0.22 V. These are consistent with the results obtained previously.[12]

To further understand the electron-transfer kinetics involved in the above quantized capacitance-charging processes, we utilized the Laviron's approach[19] in an attempt to determine the electron-transfer coefficient, α, and the rate constant, k. In this approach, the cathodic ($E_{p,c}$) and anodic ($E_{p,a}$) peak positions at various potential sweep rate rates (ν) are expressed as

$$E_{p,c} = E^{\circ} - \frac{RT}{\alpha nF} \ln\left(\frac{\alpha nF}{kRT}\right) - \frac{RT}{\alpha nF} \ln \nu \quad (2)$$

$$E_{p,a} = E^{\circ} + \frac{RT}{(1-\alpha)nF} \ln\left[\frac{(1-\alpha)nF}{kRT}\right] - \frac{RT}{(1-\alpha)nF} \ln \nu \quad (3)$$

where E° is the formal potential, and R, T, F, and n have their usual significance. Thus, plots of $E_{p,c}$ and $E_{p,a}$ vs ln ν should yield two straight lines whose slopes (s_c, and s_a) are $-RT/\alpha nF$ and $RT/(1 - \alpha)nF$, respectively. Consequently, one can determine the values of α and k from below:

$$\alpha = \frac{s_a}{s_a - s_c} \quad (4)$$

$$k = \alpha nF\nu_c/RT \text{ or } (1 - \alpha)nF\nu_a/RT \quad (5)$$

where ν_c and ν_a are the cathodic and anodic sweep rates at E_p = E°, respectively.

It has to be noted that the above approach is valid only for totally irreversible reactions for electroactive species immobilized onto an electrode surface.[19] Experimentally, this can be approximated when the difference in cathodic and anodic peak potentials (ΔE_p) > 200/n mV. Here we take the +3/+2 charging wave of the MPC adsorbed monolayer as the illustrating example. Figure 2 shows the sweep rate dependence of peak potentials, where one can see that at ν > 1.5 V/s, ΔE_p > 200 mV. Equations 2 and 3 are then applied to the experimental data, and from the linear regressions for the anodic and cathodic branches, one can estimate the value of electron-transfer coefficient, α = 0.51, indicating that the energy barrier for MPC capacitance charging is rather symmetric, whereas the rate constant (k) is approximately 10 s^{-1} (the values from the ν_c and ν_a are 9 and 11 s^{-1}, respectively), which is consistent with that obtained from impedance measurements (vide infra).

Impedance measurements (EG&G PARC 283 Potentiostat and 1025 Frequency Response Detector) were also carried out with the surface assemblies of MPCs in the same TBAP−CH$_2$Cl$_2$
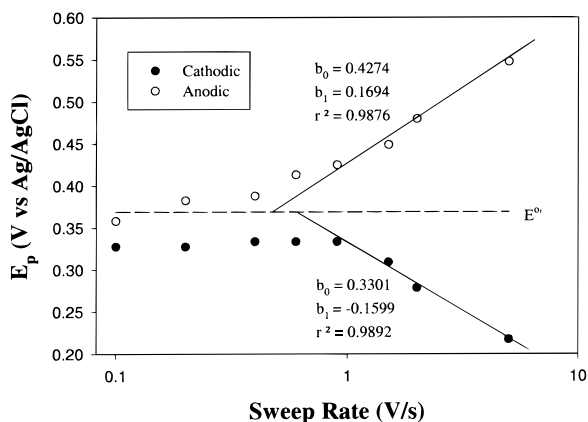
Figure 2. Laviron plot of the dependency of peak potentials on sweep rates. Peak positions determined from CV measurements (Figure 1).
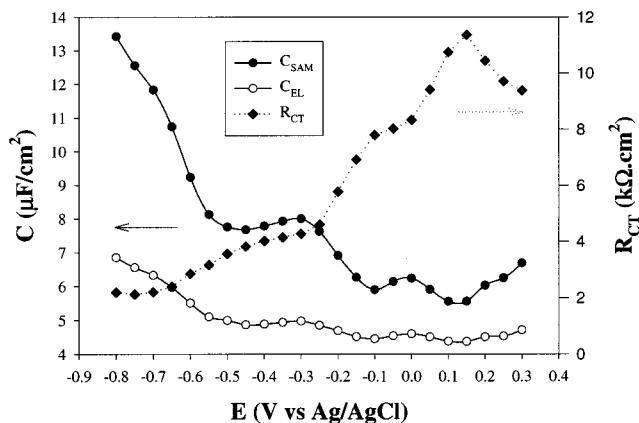

Figure 3. Variation of the double-layer capacitance of this MPC-modified electrode with applied voltage bias in the same electrolyte solution. Data were obtained from the fits of the impedance measurements ($1-100$ kHz) using the equivalent circuit in Scheme 1C. AC amplitude 10 mV.

Figure 4. Differential pulse (DPV) voltammograms of a gold electrode modified by a monolayer C6Au particles where the interparticle voids were filled by sequential adsorption of hexanethiols. The supporting electrolyte solution was aqueous 0.1 M KNO_3. Voltammetric parameters are the same as in Figure 1. Charging peaks are marked with asterisks.

proximately 50 μM). It is therefore anticipated that higher coverage might be achieved with more concentrated MPC solutions.

In addition, the electron-transfer rate constant $(k)^{21-24}$ can be estimated from the fitting parameters of the impedance spectra as well:

$$k = \frac{1}{2C_{SAM}R_{CT}} \tag{6}$$

From Figure 3, one can reach a value of k about 20 s^{-1}, which is somewhat greater than that obtained by the Larivon approach shown above.

It has to be noted that the above quantized charging behaviors were observed only in organic media so far; whereas in aqueous solutions, only featureless responses were found (not shown). This observation could also be interpreted by the above equivalent circuit (Scheme 1C). In organic solvents, as per unit electrode surface area, $C_{SAM} > C_{EL}$ (Figure 3),[12] the overall electrode double-layer capacitance is governed mainly by the adsorbed particles and the resulting current measured reflects the collective quantized charging of individual surface-immobilized MPCs; whereas, in aqueous solutions, $C_{SAM} \ll C_{EL}$,[12] thus, the electrode double-layer charging is mainly through the "naked" surface, showing classical charging features of electrode double layers.

Therefore, to observe the quantized charging properties in aqueous media, one would have to "fill" the interparticle voids with low dielectric molecules so that $C_{EL} < C_{SAM}$. Here, after the construction of MPC adlayers, the MPC-modified electrode was transferred into an ethanolic solution of 1 mM 1-hexanethiol (C6SH) for 3 h (longer times seemed to result in partial displacement of adsorbed MPCs as measured electrochemically). The electrode was then rinsed thoroughly with ethanol and dried in a N_2 stream before being transferred into an aqueous electrolyte solution for further electrochemical measurements. Figure 4 shows the resulting DPV profile in 0.1 M KNO_3. One can see that now the discrete electron-charging characteristics are rather visible, albeit not as well-defined. The peak spacings (approximately 190 mV) were somewhat smaller than those observed in organic solutions, from which the MPC capacitance in aqueous media could be estimated to be approximately 0.81 aF. The discrepancy of MPC capacitance in aqueous and organic media might be due to the depression of the hydrophobic

solution, and the spectra were fitted by the equivalent circuit proposed in Scheme 1C.[12,20] One might note that the electrode interfacial capacitance (C_{DL}) actually consists of two components (Scheme 1C), C_{SAM} and C_{EL}, which account for the contributions from the electrode surface with and without adsorbed MPCs, respectively. From Figure 3, one can see that the modulation of C_{SAM} with electrode potential appears to be in-phase with the voltammetric measurements where a maximum of C_{SAM} corresponds to a current peak at roughly the same potential, while that of the charge-transfer resistance (R_{CT}) appears to be 90° out-of-phase, as observed previously.[12] Since this C_{SAM} is the collective contributions of all surface-bound MPCs (i.e., an ensemble of nanocapacitors in parallel), the MPC surface coverage could be estimated by C_{SAM}/C_{MPC}, which is about 1.23 $\times$ 10^{-11} mol/cm^2 or 7.40 $\times$ 10^{12} molecules/cm^2 (by taking values at the PZC position). Assuming a close-packed (hexagonal) structure of the surface MPC assembly (Scheme 1B), this corresponds to a (center-to-center) interparticle distance of approximately 3.95 nm, somewhat larger than the average physical diameter of 3.5 nm (core + monolayers), representing a surface coverage of roughly 0.8 of a monolayer. This is, again, consistent with the above observations of quantized capacitance charging which suggest that the lateral resistance might be greater than that between particle and electrode. On the other hand, it has to be noted that this surface layer was obtained by self-assembling from a relatively dilute MPC solution (ap-
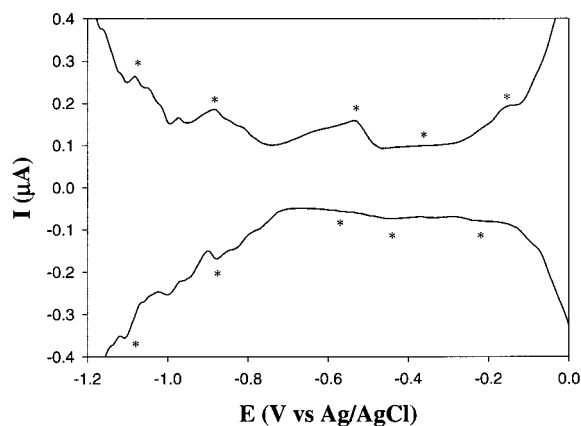
Letters

J. Phys. Chem. B, Vol. 104, No. 4, 2000 **667**

alkanethiolate layers in water, i.e., the shrinking of the effective monolayer thickness.

This experiment clearly demonstrates that the electrical properties at the electrode interface could be manipulated with relative ease by an adsorbed array of (monodisperse) MPC molecules. In addition, as the quantized capacitance charging of MPCs showed a core-size-dependent transition, manifested by a growing central gap with decreasing particle core size in the voltammetric current measurements,[11b] one might suspect that a discontinuous charge states could be achieved at an electrode surface modified by MPCs with varied sizes. This will be important, especially in the application for electron-transfer mediation in both aqueous and nonaqueous media. More detailed investigations of the MPC adsorption dynamics as well as the surface structures are currently underway and will be reported in due course.

In summary, by surface-exchange reaction and liquid extraction, surface-active nanoparticles were readily synthesized, which were then used for the construction of MPC self-assembled monolayers. It is anticipated that the above strategy will be extended to other metal nanoparticles as well (e.g., Ag, Pd, etc.),[1,25] paving the way toward the fabrication of more complicated surface nanoarchitectures.

References and Notes

(1) Markovich, G.; Leff, D. V.; Chung, S. W.; Soyez, H. M.; Dunn, B.; Heath, J. R. *Appl. Phys. Lett.* **1997**, *70*, 3107.

(2) (a) Freeman, R. G.; Grabar, K. C.; Allison, K. J.; Bright, R. M.; Davis, J. A.; Guthrie, A. P.; Hommer, M. B.; Jackson, M. A.; Smith, P. C.; Walter, D. G.; Natan, M. J. *Science* **1995**, *267*, 1629. (b) Grabar, K. C.; Smith, P. C.; Musick, M. D.; Davis, J. A.; Walter, D. G.; Jackson, M. A.; Guthrie, A. P.; Natan, M. J. *J. Am. Chem. Soc.* **1996**, *118*, 1148. (c) Lyon, L. A.; Pena, D. J.; Natan, M. J. *J. Phys. Chem. B* **1999**, *103*, 5826.

(3) (a) Peschel S.; Schmid, G. *Angew. Chem., Int. Ed. Engl.* **1995**, *34*, 1442. (b) Schmid, G.; Peschel, St.; Sawitowski, Th. *Z. Anorg. Allg. Chem.* **1997**, *623*, 719.

(4) (a) Andres, R. P.; Bein, T.; Dorogi, M.; Feng, S.; Henderson, J. I.; Kubiak, C. P.; Mahoney, W.; Osifchin, R. G.; Reinfenberger, R. *Science* **1996**, *272*, 1323. (b) Andres, R. P.; Bielefeld, J. D.; Henderson, J. I.; Janes, D. B.; Kolagunta, V. R.; Kubiak, C. P.; Mahoney, W. J.; Osifchin, R. G. *Science* **1996**, *273*, 1690.

(5) (a) Baum, T.; Bethell, D.; Brust, M. Schiffrin, D. J. *Langmuir* **1999**, *15*, 866. (b) Brust, M.; Kiely, C. J.; Bethell, D.; Schiffrin, D. J. *J. Am. Chem. Soc.* **1998**, *120*, 12367. (c) Kiely, C. J.; Fink, J.; Brust, M.; Bethell, D.; Schiffrin, D. J. *Nature* **1998**, *396*, 444.

(6) Mayya, K. S.; Sastry, M. *Langmuir* **1999**, *15*, 1902.

(7) Shenton, W.; Davis, S. A.; Mann, S. *Adv. Mater.* **1999**, *11*, 449.

(8) Yin, J. S.; Wang, Z. L. *Adv. Mater.* **1999**, *11*, 469.

(9) Fendler, J. H. *Chem. Mater.* **1996**, *8*, 1616.

(10) Feldheim, D. L.; Keating, C. D. *Chem. Rev.* **1998**, *27*, 1.

(11) (a) Ingram, R. S.; Hostetler, M. J.; Murray, R. W.; Schaaff, T. G.; Khoury, J.; Whetten, R. L.; Bigioni, T. P.; Guthrie, D. K.; First, P. N. *J. Am. Chem. Soc.* **1997**, *119*, 9279. (b) Chen, S.; Ingram, R. S.; Hostetler, M. J.; Pietron, J. J.; Murray, R. W.; Schaaff, T. G.; Khoury, J. T.; Alvrez, M. M.; Whetten, R. L. *Science* **1998**, *280*, 2098. (c) Chen, S.; Murray, R. W.; Feldberg, S. W. *J. Phys. Chem. B* **1998**, *102*, 9898. (d) Hicks, J. F.; Templeton, A. C.; Chen, S.; Sheran, K. M.; Jasti, R.; Murray, R. W.; Debord, J.; Schaaff, T. G.; Whetten, R. L. *Anal. Chem.* **1999**, *71*, 3703. (e) Pietron, J. J.; Hicks, J. F.; Murray, R. W., *J. Am. Chem. Soc.* **1999**, *121*, 5565.

(12) Chen, S.; Murray, R. W. *J. Phys. Chem. B* **1999**, *103*, 9996.

(13) Chen, S.; Murray, R. W. *Langmuir* **1999**, *15*, 682.

(14) Hostetler, M. J.; Templeton, A. C.; Murray, R. W. *Langmuir* **1999**, *15*, 3782.

(15) (a) Nuzzo, R. G.; Allara, D. L. *J. Am. Chem. Soc.* **1983**, *105*, 4481. (b) Chidsey, C. E. D.; Liu, G.-Y.; Rowntree, P.; Scoles, G. *J. Chem. Phys.* **1989**, *91*, 4421. (c) Bain, C. D.; Whitesides, G. M. *J. Am. Chem. Soc.* **1989**, *111*, 7164.

(16) (a) Brust, M.; Bethell, D.; Schiffrin, D. J.; Kiely, C. J. *Adv. Mater.* **1995**, *7*, 795. (b) Brust, M.; Bethell, D.; Nichols, R. J.; Schiffrin, D. J. *ibid.* **1999**, *11*, 737.

(17) Brust, M.; Walker, M.; Bethell, D.; Schiffrin, D. J.; Whyman, R. *J. Chem. Soc., Chem. Commun.* **1994,** 801.

(18) Schaaff, T. G.; Shafigullin, M. N.; Khoury, J. T.; Vezmar, I.; Whetten, R. L.; Cullen, W. G.; First, P. N.; Gutierrezwing, C.; Ascensio, J.; Jose-Yacaman, M. J. *J. Phys. Chem. B* **1997**, *191*, 7885.

(19) Laviron, E. *J. Electroanal. Chem.* **1979**, *101*, 19.

(20) Bard, A. J.; Faulkner, L. R. *Electrochemical Methods*; Wiley: New York, 1980; pp 352; The impedance plane arcs are well fit by semicircles as expected for Figure 1C.

(21) (a) Creager, S. E.; Wooster, T. T. *Anal. Chem.* **1998**, *70*, 4257. (b) Weber, K.; Hockett, L.; Creager, S. E. *J. Phys. Chem. B* **1997**, *101*, 8286.

(22) Smalley, J. F.; Feldberg, S. W.; Chidsey, C. E. D.; Linford, M. R.; Newton, M. D.; Liu, Y.-P. *J. Phys. Chem.* **1995**, *99*, 13141.

(23) Li, T. T. T.; Weaver, M. J. *J. Am. Chem. Soc.* **1984**, *106*, 6107.

(24) Carter, M. T.; Rowe, G. K.; Richardson, J. N.; Tender, L. M.; Terrill, R. H.; Murray, R. W. *J. Am. Chem. Soc.* **1995**, *117*, 2896.

(25) Chen, S.; Huang, K.; Stearns, J. A. *Chem. Mater.*, in press.